

- A. N. Chermahini, B. Hosseinzadeh, A. S. Beni, A. Teimouri, *Comput. Theor. Chem.* **994**, 97–104 (2012).
- A. P. Rauter et al., *Tetrahedron Asymmetry* **12**, 1131–1146 (2001).
- The full synthetic sequence from diacetone- β -glucose to epoxide **8** is presented in detail in the supplementary materials.
- Analysis of the crude reactions always showed 15 to 20% of hemiaminal present, even after prolonged exposure to reaction conditions.
- J. E. Hodge, C. E. Rist, *J. Am. Chem. Soc.* **75**, 316–322 (1953).
- E. M. Sánchez-Fernández, E. Álvarez, C. Ortiz Mellet, J. M. García Fernández, *J. Org. Chem.* **79**, 11722–11728 (2014).
- Z. Dai et al., *J. Proteome Res.* **7**, 2756–2768 (2008).
- M. J. Martin, L. J. Dorn, J. M. Cook, *Heterocycles* **36**, 157–189 (1993).
- Z. Rappaport, J. F. Liebman, Eds., *The Chemistry of Hydroxylamines, Oximes and Hydroxamic Acids* (Wiley, Chichester, UK, 2008), vol. 175.
- A. J. Lawson, *J. Chem. Soc. Chem. Commun.* **1979**, 456 (1979).
- L. E. Overman, *Angew. Chem. Int. Ed. Engl.* **23**, 579–586 (1984).
- R. M. Aranha, A. M. Bowser, J. S. Madalengoitia, *Org. Lett.* **11**, 575–578 (2009).
- See the supplementary materials for more information.
- The full synthetic sequence to 4*H*-imidazoles **29** and **30** is presented in detail in the supplementary materials.
- C. L. Perrin, T. J. Dwyer, *Chem. Rev.* **90**, 935–967 (1990).
- M. O. Lederer, F. Gerum, T. Severin, *Bioorg. Med. Chem.* **6**, 993–1002 (1998).

ACKNOWLEDGMENTS

We thank the SENS Foundation for financial support and G. Micalizio, A. de Grey, and W. Bains for helpful discussions.

SUPPLEMENTARY MATERIALS

www.sciencemag.org/content/350/6258/294/suppl/DC1
Materials and Methods
Supplementary Text
Figs. S1 to S5
Tables S1 to S11
References (28–32)
Spectral Data

6 July 2015; accepted 8 September 2015
10.1126/science.aac9655

CATALYSIS

Hydrogenation of carboxylic acids with a homogeneous cobalt catalyst

Ties J. Korstanje, Jarl Ivar van der Vlugt, Cornelis J. Elsevier,* Bas de Bruin*

The reduction of esters and carboxylic acids to alcohols is a highly relevant conversion for the pharmaceutical and fine-chemical industries and for biomass conversion. It is commonly performed using stoichiometric reagents, and the catalytic hydrogenation of the acids previously required precious metals. Here we report the homogeneously catalyzed hydrogenation of carboxylic acids to alcohols using earth-abundant cobalt. This system, which pairs $\text{Co}(\text{BF}_4)_2 \cdot 6\text{H}_2\text{O}$ with a tridentate phosphine ligand, can reduce a wide range of esters and carboxylic acids under relatively mild conditions (100°C, 80 bar H_2) and reaches turnover numbers of up to 8000.

There is great interest among the pharmaceutical and fine-chemical industries in finding more sustainable methods to reduce moieties such as esters and carboxylic acids to alcohols. In the emerging field of biomass feedstock conversion to produce high-value chemicals, the reduction of these abundantly available oxygen-containing functional groups is also of crucial importance. Traditionally, esters and carboxylic acids are reduced using stoichiometric reagents, such as aluminum- or borohydrides, but these pose an inherent safety risk and produce large amounts of waste material (1). Selective catalytic hydrogenation of esters and carboxylic acids to the corresponding alcohols could facilitate the synthesis of many products in various sectors of the chemical industry; for instance, it could facilitate the conversion of (biomass-derived) succinic acid into the bulk chemicals 1,4-butanediol, tetrahydrofuran (THF), or γ -butyrolactone, which can be used as solvents and as intermediates for the production of plastics and fibers (2). Also, numerous pharmaceuticals require a selective hydrogenation step of either an ester or a carboxylic acid moiety in their synthetic route (3).

The catalytic hydrogenation of esters and carboxylic acids is performed industrially by using heterogeneous catalysts that typically operate at

high temperatures and pressures (4). A milder enzymatic hydrogenation route using *Pyrococcus furiosus* cells has been reported recently (5). In recent years, however, much progress has also been made with using homogeneous catalysts for the hydrogenation of esters and acids under mild reaction conditions (6–8). Thus far, primarily ruthenium-based catalysts, in combination with multidentate ligands such as triphos [tridentate phosphine, $\text{CH}_2\text{C}(\text{CH}_2\text{PPh}_2)_3$] (9–12) or PNN pinners (PNN, 2-di-*tert*-butylphosphinomethyl-6-diethylaminomethylpyridine) (13–15), have been used for the hydrogenation of esters. Carboxylic acids, however, are difficult to hydrogenate in comparison with ketones and esters. Ligand protonation and resultant ligand dissociation, combined with overcoordination of the generated vacant sites at the metal center by the (bidentate) carboxylate conjugated base, result in detrimental catalyst deactivation. These pathways are especially problematic with first-row transition metals, which typically have weaker metal-ligand bonds than their second- and third-row congeners. To date, homogeneously catalyzed hydrogenation of carboxylic acids has only been achieved with two systems: a ruthenium/triphos system (16–19) and an iridium/bipyridine system (20, 21). Although these systems provide good activity and selectivity, the replacement of the scarce and expensive noble metals by cheaper, more abundant, and less toxic first-row transition metals, such as iron or cobalt, would enhance the sustainability of these hydrogenation reactions (Fig. 1). Recently,

iron-based catalysts for the hydrogenation of esters have been reported (22–24). Here we present a cobalt-based catalytic system capable of hydrogenating both esters and carboxylic acids to the corresponding alcohols, using H_2 as the reductant. The catalyst is generated in situ from a $\text{Co}(\text{BF}_4)_2 \cdot 6\text{H}_2\text{O}$ precursor and the triphos ligand, which are both commercially available, making this method highly suitable for use in practical organic synthesis and biomass conversion.

Initially, various cobalt precursors were tested, in combination with the triphos ligand, in the hydrogenation of methyl benzoate to yield benzyl alcohol and methanol. Combining methyl benzoate with 10 mole percent (mol %) of the metal precursor and the triphos ligand in distilled methanol, under 80 bar of initial H_2 pressure and at a 100°C reaction temperature, produced only minor amounts of alcohol with cobalt(III) acetylacetonate, cobalt(II) acetylacetonate, and cobalt(II) acetate (table S1). Using $\text{Co}(\text{BF}_4)_2 \cdot 6\text{H}_2\text{O}$ as the metal precursor resulted in almost full substrate conversion within 5 hours, providing the desired benzyl alcohol in excellent yield. Decreasing the catalyst loading to 5 mol % resulted in full conversion within 22 hours, with a good yield of benzyl alcohol. Lower catalyst loadings required very long reaction times (2 mol %, 94 hours) or led to lower overall activity (1 mol %). Based on this initial catalyst optimization, the substrate scope of the $\text{Co}(\text{BF}_4)_2 \cdot 6\text{H}_2\text{O}$ and triphos (Co/triphos) hydrogenation system was investigated (Table 1 and table S2). Using *tert*-butylbenzoate, an ester substrate that has low activity with many catalysts due to the steric hindrance of the *tert*-butyl group, full conversion was obtained within 5 hours. Also, with aliphatic esters such as methyl butyrate and methyl 3-*trans*-hexenoate, good yields of the fully reduced corresponding alcohol were obtained within 22 hours. Hydrogenation of γ -valerolactone, a substrate that can easily be obtained from biomass and, as such, is of interest for biomass valorization, produced 2-methyltetrahydrofuran and 1,4-pentanediol in good yields. These products have attracted attention for their respective applications as a fuel additive and as a monomer for polyester production (2). A long-chain fatty acid methyl ester and even a triglyceride could also be smoothly hydrogenated to obtain the corresponding reduced fatty alcohol in good yields, using the Co/triphos system.

Van 't Hoff Institute for Molecular Sciences, University of Amsterdam, Science Park 904, 1098 XH Amsterdam, Netherlands.
*Corresponding author. E-mail: c.j.elsevier@uva.nl (C.J.E.); b.debruin@uva.nl (B.d.B)

The successful application of the Co/triphos system for ester hydrogenation led us to investigate its efficacy in the more challenging conversion of carboxylic acids (Table 2). Using benzoic acid as the substrate, with 2.5 mol % catalyst loading and THF as the solvent (to prevent in situ esterification and

thus to ensure that the system is truly hydrogenating acids), benzyl alcohol was obtained in good yield within 22 hours. Removal of any remaining acid starting material and the majority of the catalyst can be easily accomplished by washing with a saturated aqueous sodium carbonate solution.

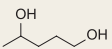
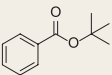
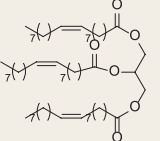
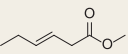
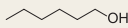
Further purification using column chromatography yielded the isolated alcohol product. Increasing the catalyst loading to 5 mol % led to full conversion after 4 hours, compared with 22 hours for methyl benzoate. This indicates that hydrogenation of carboxylic acids with the Co/triphos system outcompetes the conversion of the corresponding carboxylic esters, which is surprising, considering the difficulties associated with hydrogenating carboxylic acids in most systems. The system tolerates several functional groups, such as chlorides, fluorides, trifluoromethyls, and hydroxides, which can be used for further synthetic processing, such as C-C cross-coupling. More labile groups such as bromide, iodide, boronate, and methoxy functionalities undergo (partial) defunctionalization, but they do not hamper the reactivity (table S3).

Furthermore, the catalytic system is capable of hydrogenating a wide scope of carboxylic acid substrates, including aromatic and long- and short-chain aliphatic acids, all of which are smoothly hydrogenated to the corresponding alcohols. From a biomass viewpoint, the direct hydrogenation of levulinic acid to 2-methyltetrahydrofuran and 1,4-pentanediol is relevant, because it eliminates the need to isolate γ -valerolactone as the cyclic ester intermediate. The hydrogenation of succinic acid is also of interest, because it produces 1,4-butanediol, which is a comonomer in the production of polyesters such as polybutylene terephthalate. Furthermore, polymerization of 1,4-butanediol with (potentially biomass-derived) succinic acid constitutes a completely biomass-derived route to polybutylene succinate. In our system, short-chain acids are hydrogenated more easily than long-chain acids, which is in agreement with previous research on acid hydrogenation (20). Moreover, it is possible to reduce the liquid acids under solventless conditions, allowing low catalyst loadings (down to 0.1 mol %) for butyric acid and acetic acid, while still giving good yields of 1-butanol and ethanol, respectively. Under these conditions, esterification of the carboxylic acid starting material by the alcohol product also takes place, as demonstrated by the observation of butyl butyrate and ethyl acetate, respectively. When using formic acid or trifluoroacetic acid, neat conditions did not produce any alcohol, probably because of the high polarity of these acids. With THF as the solvent, however, a very low catalyst amount of 125 parts per million can be used for trifluoroacetic acid, while still reaching full conversion in 22 hours and giving a good yield of 50% of trifluoroethanol (the remaining mass balance consists of trifluoroethyl trifluoroacetate and an unidentified side product). Hydrogenation of formic acid in THF also proceeds smoothly, but it requires a somewhat higher catalyst loading of 0.25 to 0.5 mol %.

In comparison with the reported *P. furiosus* biocatalytic system (5), which uses a reaction temperature of 40°C and 5 bar H₂ pressure, our system generally has a lower activity and requires harsher reaction conditions; however, it is able to convert a much wider substrate scope and can obtain higher conversions of the carboxylic acid within the same period of time. Relative to our

Further purification using column chromatography yielded the isolated alcohol product. Increasing the catalyst loading to 5 mol % led to full conversion after 4 hours, compared with 22 hours for methyl benzoate. This indicates that hydrogenation of carboxylic acids with the Co/triphos system outcompetes the conversion of the corresponding carboxylic esters, which is surprising, considering the difficulties associated with hydrogenating carboxylic acids in most systems. The system tolerates several functional groups, such as chlorides, fluorides, trifluoromethyls, and hydroxides, which can be used for further synthetic processing, such as C-C cross-coupling. More labile groups such as bromide, iodide, boronate, and methoxy functionalities undergo (partial) defunctionalization, but they do not hamper the reactivity (table S3).

Table 1. Hydrogenation of esters using Co(BF₄)₂·6H₂O and triphos. General conditions used, unless otherwise noted, were 0.15 M substrate, 1:1 ratio of Co(BF₄)₂·6H₂O and triphos (mol % loading shown), distilled MeOH, 80 bar initial H₂ pressure, 100°C, 22 hours. In the substrate columns, catalyst amounts are given per ester group, and in the product columns, conversions are given with gas chromatography (GC) yields in parentheses.

Substrate	Product	Substrate	Product(s)
			 
10% (5h)	98 (95)	10%	98 (ether: 25, diol: 63)
5%	99 (79)		
			
10%	>99 (98)	10%	86 (75)
			
5%	50 (47)	10%	>75 (72)
			
10%	>99 (90)		

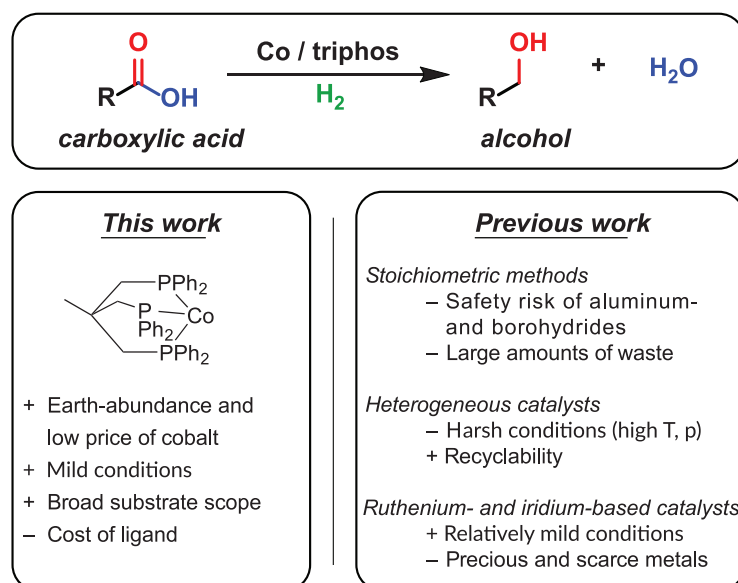


Fig. 1. Hydrogenation of carboxylic acid to alcohol. Advantages and drawbacks of previous approaches are compared with those of our catalytic system.

system, noble metal-based heterogeneous catalysts such as Ru-Sn/Al₂O₃ (25) and Pt-Re/TiO₂ (26), operating at temperatures of 240° and 130°C and pressures of 80 and 20 bar, respectively, give slightly lower conversions (82%), higher turnover numbers of stearic acid (512 and 97, respectively), and a lower selectivity due to the formation of decarboxylation and dehydration products. Furthermore, leaching of tin occurs when using the former catalyst, which is highly undesirable for a pharmaceutical application, and the Pt-Re/TiO₂ catalyst suffers from aromatic ring hydrogenation when using aromatic substrates. In comparison with previously reported homogeneous catalysts, our cobalt-based system outperforms both the ruthenium- and iridium-based systems for acid hydrogenation (19, 20): The ruthenium-based system operates at much higher temperatures (140° to 220°C) and with higher catalyst loadings (>2 mol %) than our system, and the iridium-based system requires a higher reaction temperature (120° versus 100°C) and much longer reaction times (65 versus 22 hours) to produce similar turnover numbers with acetic acid (777 for iridium versus 780 for cobalt).

To investigate the specificity of the triphos ligand, different ligand systems were tested. The tetradentate analog tetraphos [P(CH₂CH₂PPh₂)₃], known to be active in CO₂ hydrogenation in combination with cobalt (27), did not show any activity in ester hydrogenation. In addition, the combination of various bidentate phosphines with monodentate phosphines did not show any reactivity for either esters or acids. The influence of additives was investigated, but neither acid nor base had a positive effect on the reactivity in the ester hydrogenation reaction, nor did an additional reducing agent, such as zinc dust (10). The analogous cobalt precursor [Co(NCCH₃)₆](BF₄)₂, in combination with triphos, also did not show any activity in ester or acid hydrogenation under dry conditions. However, when methyl benzoate was used as the substrate, the activity was restored by adding six equivalents of water (relative to the catalyst), and [Co(THF)₆](BF₄)₂ showed carboxylic acid conversion under dry conditions. The inactivity of the [Co(NCCH₃)₆](BF₄)₂ precursor in the absence of water was probably caused by the stronger coordination of the acetonitrile ligands, which hamper reactivity under dry conditions.

The known dinuclear cobalt trihydride complex [Co₂(triphos)₂(μ-H)₃](BF₄)₂ was found to be inactive in this reaction. The inactive cobalt precursor Co(OAc)₂·4H₂O (OAc, acetate) could be activated by the addition of two equivalents of BF₃·OEt₂ (OEt₂, diethylether) or by the addition of various noncoordinating salts, such as HBF₄, NaSBF₆, or LiB(C₆F₅)₄. In contrast, the addition of NaBF₄, NaPF₆, or NaBPh₄ did not provide this activating effect. The addition of BF₃·OEt₂ or HBF₄ however, does not improve the activity in the case of the Co(BF₄)₂·6H₂O precursor. Furthermore, the addition of other Lewis acids, such as scandium (III) triflate or iron(III) chloride, had a detrimental effect on the reactivity of the Co/triphos system. This indicates that a noncoordinating anion is required to provide catalytic activity, although

further research is required to completely explain the observed counterion effect.

To further investigate the reaction mechanism, we performed partial poisoning studies using TEMPO (2,2,6,6-tetramethylpiperidine-1-oxyl) as a radical inhibitor and TMTU (tetramethylthiourea) as a strongly binding poison (28). With both reagents, the reaction was completely inhibited by one equivalent per catalyst, and for TMTU, only half an equivalent was sufficient (fig. S1). This suggests that TMTU deactivates two cobalt centers, either by acting as a bridging poison ligand or by acting on a dinuclear cobalt species, whereas TEMPO poisons a monomeric cobalt species. Furthermore, this result excludes the formation of nanoparticles

as the active catalyst, because this would require a much lower amount of poison for full inhibition of the catalysis (29). This result is consistent with a mercury poison test, which did not show any considerable inhibition of the catalysis.

We studied the reaction further by means of high-resolution electron spray ionization mass spectrometry (ESI-MS). Using benzoic acid as the substrate, a catalytic sample was analyzed after 1 hour of reaction time; the major signal detected (mass/charge ratio = 804.1875) has a mass consistent with that of a [Co(triphos)(benzoate)]⁺ species (fig. S2). The same species was detected upon separately mixing the cobalt precursor, triphos, and benzoic acid in a 1:1:1 ratio and heating

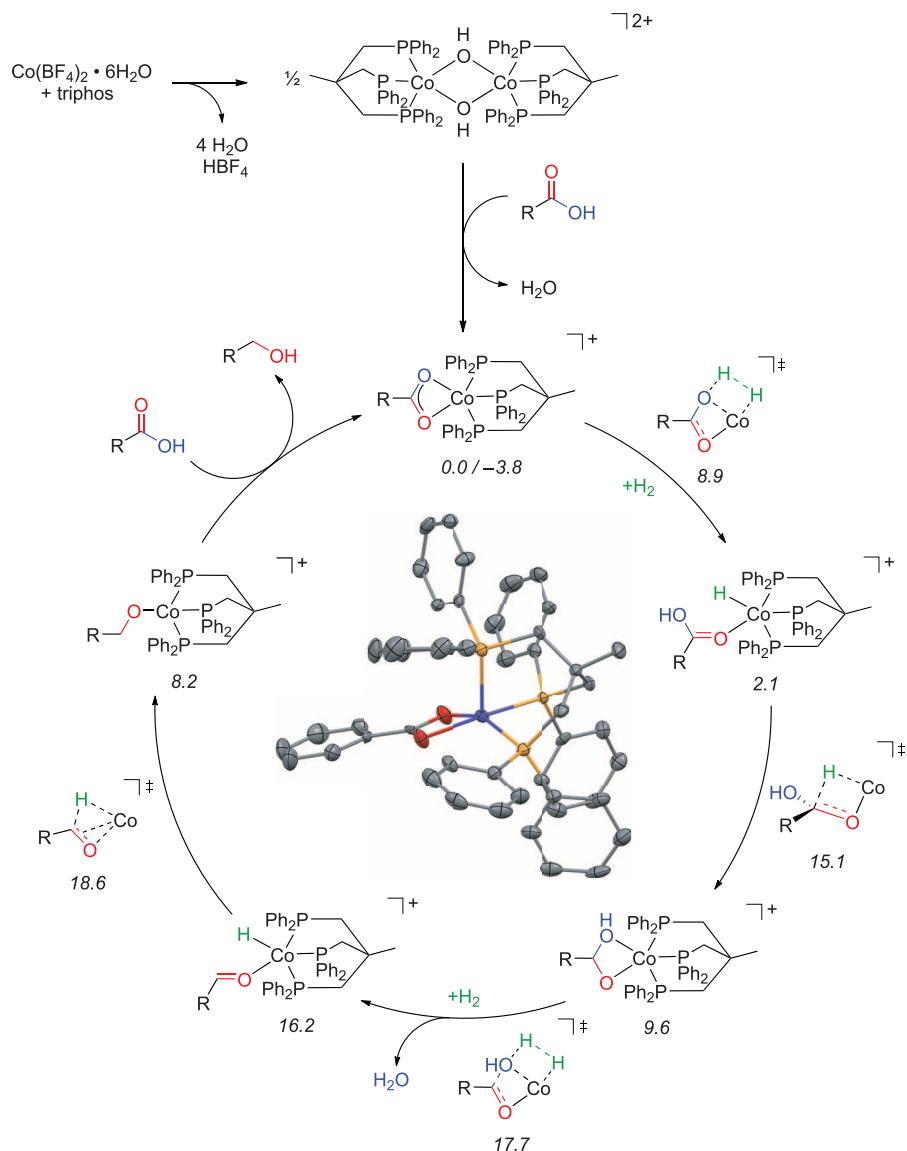


Fig. 2. Proposed mechanism for the Co/triphos-catalyzed hydrogenation of carboxylic acids to alcohols. BF₄ anions are omitted for clarity. The central area shows the crystal structure of the proposed resting state, [Co(triphos)(κ²-OOCPh)]⁺. The numbers below the structures indicate the relative enthalpies (kcal mol⁻¹) at 373 K, obtained from dispersion-corrected density functional theory (DFT-D3), using the BP86 functional, def2-TZVP basis set, and Grimme's version 3 dispersion corrections (disp3). Colors in the central structure correspond to cobalt (blue), oxygen (red), phosphorus (yellow), and carbon (gray).

this mixture briefly under an inert atmosphere. Because ESI-MS does not provide information on the oxidation state, we also performed in situ electron paramagnetic resonance (EPR) spectroscopy. The catalytic reaction was carried out in a high-pressure EPR tube, using 2-methyltetrahydrofuran as the solvent (to obtain a good glass) and 15 bar of H₂ pressure, followed by rapid cooling of the reaction mixture from 100° to -198°C (76 K) after 2 hours of reaction time. The EPR tube was subsequently cooled to 20 K in the EPR cavity to record the EPR spectrum. Two signals were observed: a broad signal, arising from a high-spin species (electron spin, $S = 3/2$) and a well-defined signal from a low-spin species ($S = 1/2$) with a complex hyperfine coupling pattern due to coupling with cobalt (nuclear spin, $I = 7/2$) and three phosphorus atoms ($I = 1/2$) (fig. S3). The high-spin species originated from a small excess amount of Co(BF₄)₂·6H₂O, whereas the low-spin species

produced an identical signal to that of an independently prepared 1:1:1 mixture of Co(BF₄)₂·6H₂O, triphos, and benzoic acid (fig. S2). This confirms the results obtained by ESI-MS and also shows that the cobalt center in this species remains in the +2 oxidation state. Based on these results, we propose the mechanism depicted in Fig. 2.

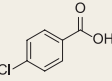
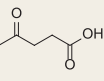
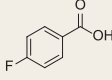
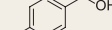
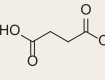
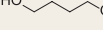
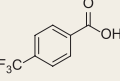
The proposed mechanism starts with the formation of a precatalytic species, [Co₂(triphos)₂(μ-OH)₂](BF₄)₂, which is known to form spontaneously when Co(BF₄)₂·6H₂O and triphos are mixed (30). This dimer is split by the substitution of the hydroxyl ligand for an alkanooate, producing the catalytically active species [Co(triphos)(alkanoate)] BF₄, which is observed in EPR and ESI-MS and is known to be a stable species (30). By means of slow vapor diffusion of diethyl ether into a CH₂Cl₂ solution of the complex, we were also able to obtain single crystals that enabled x-ray crystal structure determination of this species as the

BPh₄ salt. The complex was prepared by mixing Co(BF₄)₂·6H₂O, triphos, and benzoic acid in a 1:1:1 ratio in THF, followed by the addition of NaBPh₄ in a 10-fold excess amount. The x-ray crystal structure (Fig. 2 and table S5) shows the expected bidentate (κ²) binding mode of the benzoate and a slightly distorted square pyramidal structure around the cobalt center [$\tau = 0.11$ (37)], as expected for a low-spin cobalt(II) species. This species produces the same EPR spectrum as the catalytic mixture, confirming the Co(triphos)(κ²-alkanoate) species as the resting state, but it was found to be inactive in catalysis because of the presence of the BPh₄ anion [which has a deactivating effect on catalysis, as we also observed when NaBPh₄ was added to the catalytically active 1:1 mixture of triphos and Co(BF₄)₂·6H₂O].

From this Co(triphos)(κ²-alkanoate) species, we propose that initial heterolytic hydrogen splitting occurs over the Co-O bond, followed by the migratory insertion of the hydride into the carbonyl carbon and a second heterolytic hydrogen splitting step over the cobalt(II) hydroxyalkanoate intermediate, thereby expelling one equivalent of water and producing the [Co(triphos)(H)(aldehyde)]⁺ species (32). A final hydride migration step, followed by proton transfer and ligand exchange with another carboxylic acid substrate, gives the desired alcohol and regenerates the active catalyst. This mechanism fits the ESI-MS and EPR results that show [Co(triphos)(OOCR)]⁺ as the resting state under catalytic conditions, and it also correlates well with the quantitative poisoning studies. The proposed mechanism is also supported by density functional theory (DFT) calculations (performed on the complete system, using acetic acid as the substrate; Fig. 2 and figs. S4 and S5), showing that the (lowest-energy) resting state is the Co(triphos)(κ²-alkanoate) species. The overall calculated reaction barrier is 18.6 kcal mol⁻¹, which is a reasonable energy barrier for a reaction proceeding smoothly at 100°C. The rate-determining transition state involves hydride migration to the coordinated aldehyde, whereafter energetically favorable steps occur involving proton transfer and exchange of the product for a carboxylic acid substrate, thus resulting in an overall mildly exothermic reaction (-3.8 kcal mol⁻¹).

The results presented here describe the first catalytic system based on a cheap and abundant first-row transition metal that is capable of hydrogenating carboxylic acids to the corresponding alcohols, using molecular hydrogen as the reductant. Insight into the mechanism of this system was obtained by means of ESI-MS, in situ EPR, x-ray crystallography, and DFT calculations, all of which support a Co(triphos)(κ²-alkanoate) resting state. The DFT calculations suggest a mechanism that involves heterolytic H₂ splitting over cobalt(II) alkanooate and cobalt(II) hydroxyalkanoate intermediates as key steps in the catalytic cycle.

Table 2. Hydrogenation of carboxylic acids using Co(BF₄)₂·6H₂O and triphos. General conditions used, unless otherwise noted, were 0.15 M substrate, 1:1 ratio of Co(BF₄)₂·6H₂O and triphos (mol % loading shown), distilled THF, 80 bar initial H₂ pressure, 100°C, 22 hours. In the substrate columns, catalyst amounts are given per acid group, and in the product columns, conversions are shown with GC yield/isolated yield in parentheses.

Substrate	Product	Substrate	Product(s)	Substrate	Product
					
5% (4h)	>85 (65)	2.5%	>99 (71)	5%	95 (92)
2.5%	>85 (62 / 39)				
			 		
5%	>99 (82 / 70)	10%	>99 (ether: 14, diol: 47)	0.25%*	94 (81)
				0.1%*	78 (48 [‡])
			 		
5%	>99 (96 / 84)	2.5%	>85 (lactone: 23, diol: 61)	0.5%	>99 (76)
				0.25%	56 (22 [§])
					
5%	98 (98 / 82)	5%	>99 (95)	125 ppm	97 (50)
		0.1%*	53 (17 / 5 [†])		
					
5%	>90 (89 / 66)				

*Neat conditions. †36% GC yield and 24% isolated yield of butyl butyrate obtained. Isolated yields shown here are the amounts present in the isolated mixture of 1-butanol and butyl butyrate, because it proved difficult to separate these compounds by distillation (probably because of azeotrope formation). ‡31% ethyl acetate obtained. §29% methyl formate formed. ||Based on fluorine-19 nuclear magnetic resonance. Mass balance is completed by an unknown side product.

REFERENCES AND NOTES

- J. Seyden-Penne, *Reductions by the Almino- and Borohydrides in Organic Synthesis* (Wiley-VCH, New York, ed. 2, 1997).
- T. Weply, G. Petersen, Eds., *Top Value Added Chemicals From Biomass, Volume 1—Results of Screening for Potential*

Candidates from Sugars and Synthesis Gas (U.S. Department of Energy, Oak Ridge, TN, 2004); available at www.nrel.gov/docs/fy04osti/35523.pdf.

- J. Magano, J. R. Durnez, *Org. Process Res. Dev.* **16**, 1156–1184 (2012).
- T. Turek, D. L. Trimm, N. W. Cant, *Catal. Rev.* **36**, 645–683 (1994).
- Y. Ni, P.-L. Hagedoorn, J.-H. Xu, I. W. C. E. Arends, F. Hollmann, *Chem. Commun. (Camb.)* **48**, 12056–12058 (2012).
- P. A. Dub, T. Ikariya, *ACS Catal.* **2**, 1718–1741 (2012).
- S. Werkmeister, K. Junge, M. Beller, *Org. Process Res. Dev.* **18**, 289–302 (2014).
- J. Pritchard, G. A. Filonenko, R. van Putten, E. J. M. Hensen, E. A. Pidko, *Chem. Soc. Rev.* **44**, 3808–3833 (2015).
- H. T. Teunissen, C. J. Elsevier, *Chem. Commun. (Camb.)* **1997**, 667–668 (1997).
- H. T. Teunissen, C. J. Elsevier, *Chem. Commun. (Camb.)* **1998**, 1367–1368 (1998).
- M. C. van Engelen, H. T. Teunissen, J. G. de Vries, C. J. Elsevier, *J. Mol. Catal. Chem.* **206**, 185–192 (2003).
- Y. Li, C. Topf, X. Cui, K. Junge, M. Beller, *Angew. Chem. Int. Ed.* **54**, 5198–5200 (2015).
- J. Zhang, G. Leitius, Y. Ben-David, D. Milstein, *Angew. Chem. Int. Ed.* **45**, 1113–1115 (2006).
- J. Zhang, E. Balaraman, G. Leitius, D. Milstein, *Organometallics* **30**, 5716–5724 (2011).
- E. Balaraman, E. Fogler, D. Milstein, *Chem. Commun. (Camb.)* **48**, 1111–1113 (2012).
- M. Kilner, D. V. Tyers, S. P. Crabtree, M. A. Wood, World Intellectual Property Organization (WO) Patent 03/093208 (2003).
- M. A. Wood, S. P. Crabtree, D. V. Tyers, WO Patent 2005/051875 (2005).
- F. M. A. Geilen, B. Engendahl, M. Hölscher, J. Klankermayer, W. Leitner, *J. Am. Chem. Soc.* **133**, 14349–14358 (2011).
- T. vom Stein *et al.*, *J. Am. Chem. Soc.* **136**, 13217–13225 (2014).
- T. P. Brewster, A. J. M. Miller, D. M. Heinekey, K. I. Goldberg, *J. Am. Chem. Soc.* **135**, 16022–16025 (2013).
- K. Goldberg, D. M. Heinekey, J. M. Mayer, A. J. M. Miller, T. P. Brewster, WO Patent 2014/130714 (2014).
- T. Zell, Y. Ben-David, D. Milstein, *Angew. Chem. Int. Ed.* **53**, 4685–4689 (2014).
- S. Werkmeister *et al.*, *Angew. Chem. Int. Ed.* **53**, 8722–8726 (2014).
- S. Chakraborty *et al.*, *J. Am. Chem. Soc.* **136**, 7869–7872 (2014).
- M. Toba *et al.*, *Appl. Catal. A Gen.* **189**, 243–250 (1999).
- H. G. Manyar *et al.*, *Chem. Commun. (Camb.)* **46**, 6279–6281 (2010).
- C. Federsel, C. Ziebart, R. Jackstell, W. Baumann, M. Beller, *Chemistry* **18**, 72–75 (2012).
- R. M. Drost *et al.*, *ChemCatChem* **7**, 2095–2107 (2015).
- R. H. Crabtree, *Chem. Rev.* **112**, 1536–1554 (2012).
- C. Mealli, S. Midollini, L. Sacconi, *Inorg. Chem.* **14**, 2513–2521 (1975).
- A. W. Addison, T. N. Rao, J. Reedijk, J. van Rijn, G. C. Verschoor, *J. Chem. Soc., Dalton Trans.* **1984**, 1349–1356 (1984).
- A similar structure with a PEt_3 group instead of the acetaldehyde, $[\text{Co}(\text{triphos})(\text{H})(\text{PEt}_3)]\text{BPh}_4$ is described in (33).
- C. Bianchini, D. Masi, C. Mealli, A. Mei, M. Sabat, *Gazz. Chim. Ital.* **116**, 201–204 (1986).

ACKNOWLEDGMENTS

This research was performed within the framework of the CatchBio program. The authors gratefully acknowledge the support of the Smart Mix Program of the Netherlands Ministry of Economic Affairs and the Netherlands Ministry of Education, Culture and Science. We thank E. Zuidinga for ESI-MS analysis and L. Lefort and P. Alsters for useful discussions. The supplementary crystallographic data for this structure can be obtained free of charge from The Cambridge Crystallographic Data Centre (CCDC) at www.ccdc.cam.ac.uk/getstructures (CCDC number 1420869).

SUPPLEMENTARY MATERIALS

www.sciencemag.org/content/350/6258/298/suppl/DC1

Materials and Methods

Figs. S1 to S39

Tables S1 to S5

References (34–46)

Cartesian Coordinates (XYZ Format) for All Calculated Structures

3 April 2015; accepted 8 September 2015

10.1126/science.aaa8938

SEPARATION MEMBRANES

CO₂ capture from humid flue gases and humid atmosphere using a microporous coppersilicate

Shuvo Jit Datta,¹ Chutharat Khumnoon,¹ Zhen Hao Lee,¹ Won Kyung Moon,¹ Son Doaco,¹ Thanh Huu Nguyen,¹ In Chul Hwang,¹ Dohyun Moon,² Peter Oleynikov,³ Osamu Terasaki,^{3,4,5} Kyung Byung Yoon^{1*}

Capturing CO₂ from humid flue gases and atmosphere with porous materials remains costly because prior dehydration of the gases is required. A large number of microporous materials with physical adsorption capacity have been developed as CO₂-capturing materials. However, most of them suffer from CO₂ sorption capacity reduction or structure decomposition that is caused by co-adsorbed H₂O when exposed to humid flue gases and atmosphere. We report a highly stable microporous coppersilicate. It has H₂O-specific and CO₂-specific adsorption sites but does not have H₂O/CO₂-sharing sites. Therefore, it readily adsorbs both H₂O and CO₂ from the humid flue gases and atmosphere, but the adsorbing H₂O does not interfere with the adsorption of CO₂. It is also highly stable after adsorption of H₂O and CO₂ because it was synthesized hydrothermally.

Efforts to curtail the increase in atmospheric CO₂ concentrations rely on the development of economical methods of capturing CO₂ from flue gas and the atmosphere (1–5). One possible approach involves capture of CO₂ by physical adsorption on microporous materials that have high surface areas. To date, various materials that have high CO₂ sorption capabilities at 298 K have been developed. They include zeolites (6–10), metal-organic frameworks (MOFs) (11–16), and zeolitic imidazolate frameworks (17, 18). However, these materials require the incoming gas stream to be completely dehydrated, as water causes a drastic reduction in the CO₂ sorption capabilities (19, 20) or may even promote their decomposition (13, 14). Although such moisture-sensitive CO₂ sorbents can still be used to capture CO₂ directly from nonpretreated humid flue gases by charging the column with a water-sorbing layer before the CO₂-sorbing layer, the use of a single moisture-insensitive layer would be preferable (4, 5, 21).

Only a limited number of materials meeting this requirement have been discovered, and these substances can only adsorb small to moderate amounts of CO₂ from humid flue gas (13, 14, 18–20). Furthermore, most flue gases are hot, with temperatures ranging between 373 and 403 K at the point they are released into the atmosphere. Therefore, thermal stability under humid conditions is another key property.

Using a gel consisting of sodium silicate and copper sulfate, we synthesized microporous coppersilicate crystals of uniform size and shape (see supplementary materials). The crystals, which we call SGU-29, have a square bipyramid crystal morphology, which suggests that each crystal has pseudo-four-fold symmetry along the axis (assigned later as the *c* axis) from the center of the square to the top of the pyramid. Two typical scanning electron microscopy (SEM) images with different crystal sizes are shown in Fig. 1A and the inset. The determined chemical formula was Na₂CuSi₅O₁₂. Almost all reflections observed in the x-ray powder diffraction pattern matched well with those of ETS-10 (22, 23) and AM-6 (fig. S1) (24, 25). The crystals are stable in air up to 550°C (fig. S2). The effective magnetic moment of Cu (fig. S3A) confirmed that the oxidation state of Cu is 2+. The electron spin resonance spectrum of SGU-29 showed that the electron spins on Cu²⁺ ions are strongly coupled (fig. S3B). Characteristic features observed by transmission electron microscopy (TEM) can be summarized as follows: (i) In the high-resolution TEM (HRTEM) image taken along the 110 direction (parallel to the channel direction; Fig. 1B), large bright ellipses are arranged horizontally with a period of 14.7 Å with a dark contrast observed between any two neighboring ellipses. Simultaneously, a horizontal row of small white dots arranged in a zigzag manner can also be noticed between the successive arrays of ellipses. The bright contrast of ellipses and small dots corresponds to large and small pores, respectively. The large pores resemble channels formed by 12-membered rings judging from their sizes. These pores belong to single layers that are marked as A, B, C, and D. (ii) There is a horizontal shift by one-quarter of the ellipses between successive layers either to the right in the upper part of the image forming ABCD stacking sequence or

¹Korea Center for Artificial Photosynthesis, Department of Chemistry, Sogang University, Seoul 121-742, Korea. ²Pohang Accelerator Laboratory, Pohang University of Science and Technology, Pohang 790-784, Korea. ³Department of Materials and Environmental Chemistry, Stockholm University, SE-106 91 Stockholm, Sweden. ⁴Graduate School of EEWs, KAIST, Daejeon 305-701, Korea. ⁵School of Physical Science and Technology, ShanghaiTech University, Shanghai 201210, China. *Corresponding author. E-mail: yoomb@sogang.ac.kr

This copy is for your personal, non-commercial use only.

If you wish to distribute this article to others, you can order high-quality copies for your colleagues, clients, or customers by [clicking here](#).

Permission to republish or repurpose articles or portions of articles can be obtained by following the guidelines [here](#).

The following resources related to this article are available online at www.sciencemag.org (this information is current as of October 15, 2015):

Updated information and services, including high-resolution figures, can be found in the online version of this article at:

<http://www.sciencemag.org/content/350/6258/298.full.html>

Supporting Online Material can be found at:

<http://www.sciencemag.org/content/suppl/2015/10/14/350.6258.298.DC1.html>

This article appears in the following **subject collections**:

Chemistry

<http://www.sciencemag.org/cgi/collection/chemistry>